Journal of Nuclear Materials 406 (2010) 304–316

Contents lists available at ScienceDirect

Journal of Nuclear Materials

journal homepage: www.elsevier.com/locate/jnucmat

Osmosis-induced swelling of Eurobitum bituminized radioactive waste in constant total stress conditions

E. Valcke [a,*], A. Marien [a], S. Smets [a], X. Li [b], N. Mokni [c], S. Olivella [c], X. Sillen [d]

[a] Waste and Disposal Expert Group, The Belgian Nuclear Research Centre (SCK·CEN), Boeretang 200, 2400 Mol, Belgium
[b] EIG EURIDICE, Boeretang 200, 2400 Mol, Belgium
[c] Department of Geotechnical Engineering and Geosciences, Universidad Politécnica de Catalunya (UPC), Spain
[d] ONDRAF/NIRAS, Kunstlaan 14, 1210 Brussel, Belgium

ARTICLE INFO

Article history:
Received 2 June 2010
Accepted 31 August 2010

ABSTRACT

In geological disposal conditions, contact of Eurobitum bituminized radioactive waste, which contains high amounts of the hygroscopic and highly soluble $NaNO_3$, with groundwater will result in water uptake and swelling of the waste, and in subsequent leaching of the embedded $NaNO_3$ and radionuclides. The swelling of and the $NaNO_3$ leaching from non-radioactive Eurobitum samples, comprised between two stainless steel filters and in contact with 0.1 M KOH, was studied in restricted (semi-confined) swelling conditions, *i.e.* under a constant total stress, or counterpressure, of 2.2, 3.3, or 4.4 MPa (*i.e.* oedometer conditions). Four tests were stopped after hydration times between 800 and 1500 days, and the samples were analyzed by micro-focus X-ray Computer Tomography (μCT) and by Environmental Scanning Electron Microscopy (ESEM). The complete set of data enabled a consistent interpretation of the observations and lead to an improved understanding of the phenomenology of the water uptake, swelling, and $NaNO_3$ leaching in restricted swelling conditions. Under the studied conditions, the bituminous matrix surrounding the $NaNO_3$ crystals and pores with $NaNO_3$ solution behaved as a highly efficient semi-permeable membrane, *i.e.* osmotic processes occurred. In the main part of the leached layers, a high average $NaNO_3$ concentration and related to this a high osmotic pressure prevailed, explaining why in the studied range the swelling was not measurably affected by the counterpressure. At the interface with the stainless steel filters, a low permeable re-compressed bitumen layer was formed, contributing to the slow release of $NaNO_3$ compared to the water uptake rate. A fully coupled Chemo-Hydro-Mechanical (CHM) constitutive model has been developed that integrates the key processes involved and that reproduces satisfactorily the results; this is presented in another work. Combination of the experimental and the modelling study allow to conclude that under semi-confined conditions the swelling of the bituminized waste, and its evolution with time, is the result of several transient processes (salts dissolution, diffusion of salts and water, advection, creep, involving a low permeability material with evolving thickness and properties) that moreover are non-linear and strongly coupled.

1. Introduction

Eurobitum intermediate level bituminized radioactive waste has been produced at the EUROCHEMIC/BELGOPROCESS reprocessing facility (Mol-Dessel, Belgium), to immobilise precipitation sludge and evaporator concentrates originating from the chemical reprocessing of spent nuclear fuel and cleaning of high level waste storage tanks. Eurobitum consists of ~60 weight% (wt%) of 'hard' (also called 'blown' or 'oxidized') bitumen (Mexphalt R85/40) and ~40 wt% of waste. $NaNO_3$ and $CaSO_4$ are the most abundant salts and make up respectively 20–30 wt% and 4–6 wt% of the bituminized waste (BW). The waste further contains CaF_2, $Ca_3(PO_4)_2$, $Ni_2[(Fe, Mn)(CN)_6]$, and oxides and hydroxides of Fe, Zr, and Al (4–10 wt%). Radionuclides are estimated to be present but for some 0.2 wt% at most [1,2]. All these salts, precipitates, and (hydr)oxides are finely dispersed in a matrix of bitumen (Fig. 1).

The current reference solution pursued by the Belgian Agency for the Management of Radioactive Waste and Fissile Materials (ONDRAF/NIRAS) envisages the direct underground disposal of Eurobitum in a geologically stable clay formation [3]. The Boom Clay, which is a 30–35 million years old and ~100 m thick marine sediment, is presently being studied as a reference host formation because of its favourable properties to limit and delay the migration of the leached radionuclides over extended periods of time [4]. When not disturbed, the Boom Clay will thus delay and spread

* Corresponding author. Tel.: +32 14333133; fax: +32 14323553.
E-mail addresses: evalcke@sckcen.be (E. Valcke), xli@sckcen.be (X. Li), nadia.mokni@upc.edu (N. Mokni), sebastia.olivella@upc.edu (S. Olivella), x.sillen@nirond.be (X. Sillen).

0022-3115/$ - see front matter © 2010 Elsevier B.V. All rights reserved.
doi:10.1016/j.jnucmat.2010.08.060

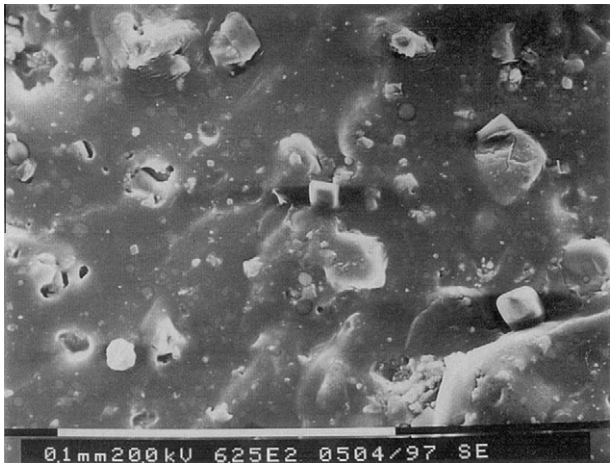

Fig. 1. SEM photograph of Eurobitum bituminized radioactive salts. Both smaller (∅2–3 μm) and larger (∅15–20 μm) $NaNO_3$ crystals, as well as other salts, precipitates, and (hydr)oxides, are homogeneously dispersed in a matrix of bitumen. Note that the bitumen matrix is almost 'saturated' with the waste substances. Energy-Dispersive X-ray (EDX) analyses show that even the places that apparently consist of 'pure' bitumen contain $NaNO_3$ and $CaSO_4$.

in time the migration of the radionuclides, allowing the majority to decay before reaching the aquifers. Several 220 l drums, filled with ~170 l of Eurobitum, would be grouped in thick-walled concrete 'secondary' containers, which in turn would be placed in concrete-lined disposal galleries that are excavated at mid-depth in the clay layer. The remaining voids between the containers would be backfilled with a cement-based material.

A good understanding of the long-term behavior of Eurobitum in underground disposal conditions is an absolute prerequisite in view of its safe geologic disposal. Amongst the processes of concern, the interaction of the bituminized waste with clay pore water is of particular importance [2,5]. $NaNO_3$ is a very hygroscopic and deliquescent salt: it will strongly absorb large amounts of water or water vapour from the environment it is exposed to, resulting in the formation of an aqueous solution (*i.e.* deliquescence) [6]. The bitumen that surrounds the salt crystals has a very low permeability to water, but its ability to restrict the movement of dissolved ions even more makes it behave as a highly efficient semi-permeable membrane [7,8]. As a result, contact of the bituminized waste with water will result in an osmosis-induced swelling of the waste [9–14]. If (further) swelling is hindered, the swelling Eurobitum will exert a high 'osmotic' (*i.e.* osmosis-induced) pressure on its surroundings [10,14–16] (see Appendix A). In addition to the dissolution of $NaNO_3$, anhydrous calcium sulfate ('natural anhydrite'; solubility ~0.015 mol/L (M); density ~2.96 g/ml) can recrystallise with 0.5 water molecules to 'Paris Plaster' (solubility ~0.21 M; density ~2.74 g/ml) or with two water molecules to gypsum (solubility ~0.014 M; density ~2.32 g/ml), also resulting in a volume and/or pressure increase. High swelling-induced deformation and stresses could thus lead to a mechanical disturbance and possibly damage of the surrounding host formation [17], of which the consequences in terms of barrier performance have to be assessed.

To better understand these processes, and to enable to predict the long-term behavior of Eurobitum in underground disposal conditions, ONDRAF/NIRAS launched a large research programme. At the Belgian Nuclear Research Centre SCK·CEN water uptake experiments in constant volume and constant total stress (or: constant counterpressure) conditions are performed, and the influence of several parameters ($NaNO_3$ content in the BW and in the leachant, and degree of ageing) is investigated. Simultaneously, the International Centre for Numerical Methods and Engineering (CIMNE, Polytechnical University of Cataluña, Barcelona, Spain) started developing a fully coupled chemo-hydro-mechanical constitutive model for Eurobitum that considers the coupled osmotic flow and ultrafiltration [18]. The first results of the experimental programme were reported in [14,16]. In this paper, we report new experimental results on swelling, $NaNO_3$ leaching, and characterisation of leached samples, for the constant total stress tests. Before proceeding, we briefly summarize the present insights in the phenomenology of the water uptake and swelling in free swelling conditions.

2. Phenomenology of the water uptake and swelling in free swelling conditions

The phenomenology of the water uptake, swelling, and salt leaching processes in free swelling conditions is now reasonably well understood [8,10–13]. For a BW like Eurobitum, with a waste loading of ~40 wt% and with a $NaNO_3$ content between 20 and 30 wt%, the processes occurring in unconfined conditions, *i.e.* where free swelling is possible, can be described in a simple way by considering a binary mixture of bitumen and $NaNO_3$ (Fig. 2). In contact with water, the $NaNO_3$ salt crystals at the surface (see also Fig. 1), which are not covered by a layer of bitumen, will dissolve rapidly in the contacting solution. Water will also diffuse slowly through the bitumen that surrounds the $NaNO_3$ crystals in the layer just underneath the outer bitumen layer – which (initially) acts as a highly efficient semi-permeable membrane[1] – and start to dissolve these $NaNO_3$ crystals. This results in the formation of pores filled with a mixture of undissolved $NaNO_3$ in contact with a saturated $NaNO_3$ solution (7.8457 mol/dm^3 at 25 °C, [19]). The water activity[2] of this mixture, as well as the water activity of a saturated $NaNO_3$ solution, is 0.74. As the volume of the $NaNO_3$–H_2O mixture is larger than that of $NaNO_3$, this layer of the BW swells.

Because the diffusion of water through the bitumen in the BW is a slow process, most of the water that is taken up further by the BW stays in the 'first' layer of pores, to dissolve the remaining $NaNO_3$ crystals and, in a next step, to dilute the saturated $NaNO_3$ solution. As a result, big pores filled with gradually less concentrated $NaNO_3$ solution – and thus with gradually increasing water activities – appear in the outer BW layer [12]. A small part of the water that is taken up diffuses deeper into the BW, until it reaches the next $NaNO_3$ crystals to be dissolved and diluted, contributing in turn to the swelling. This fraction of water diffusing deeper into the BW increases as the water activity in the first layer becomes higher than 0.74, which is achieved when all $NaNO_3$ crystals are dissolved and the saturated $NaNO_3$ solution starts to dilute.

The swelling of the BW as a result of the water uptake modifies, by the high stretching of the bitumen, the membrane properties of the surrounding bitumen (rather: bituminous matrix, see below), making it gradually more permeable to the dissolved salts, *i.e.* the bitumen behaves increasingly less as a highly efficient semi-permeable membrane. In addition, at high swelling degrees, the $NaNO_3$ solution filled pores may become interconnected. This way, a continuously growing permeable layer consisting of connected pores is created. As a result, $NaNO_3$ can leach from the BW. It is to be noted that it is likely that in BW the omnipresence of the waste compounds (soluble and sparingly soluble salts, (hydr)oxides, ... ; Fig. 1) creates already from the start a low-porosity

[1] The efficiency of a material to behave as a semi-permeable membrane, *i.e.* the osmotic efficiency, is calculated as the ratio of the measured osmotic pressure and the theoretical osmotic pressure if the material were an ('100%') ideal semi-permeable membrane (*e.g.* S.J. Fritz, Ideality of clay membranes in osmotic processes: a review, Clays and Clay Minerals 34 (2) (1986) 214–223). Accordingly, a highly efficient semi-permeable material refers to a material with a high osmotic efficiency.

[2] The water activity is defined as the ratio of the water vapour pressure of a salt solution and the water vapour pressure of pure water. This value is temperature-dependent.

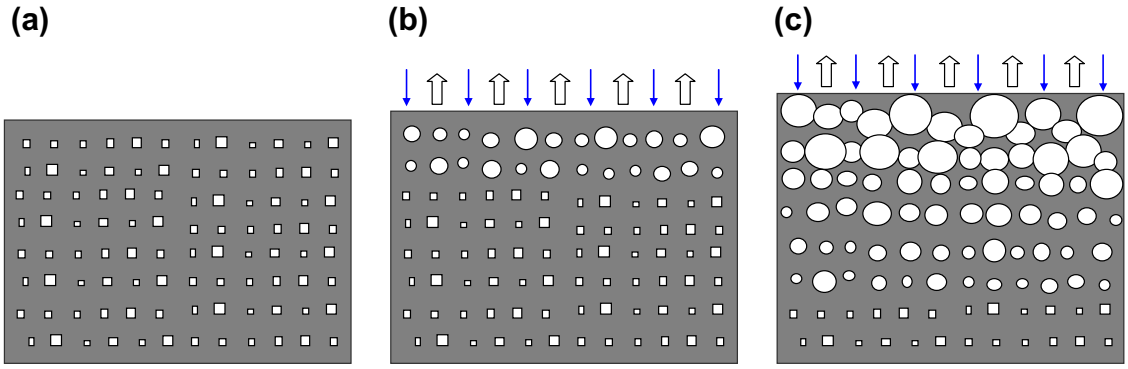

Fig. 2. Simplified schematic representation of the water uptake and swelling in a binary bitumen – $NaNO_3$ mixture in free swelling conditions. (a) Dry mixture of bitumen and $NaNO_3$ crystals. (b) Mixture in which in the first layers the $NaNO_3$ crystals are partially or completely dissolved (to an oversaturated, saturated, or undersaturated solution). (c) Mixture with layers of large pores with (more) diluted solution, and small pores with (more) concentrated ((over, under)saturated) $NaNO_3$ solution. □ = dry $NaNO_3$ crystal, ○ = pore with $NaNO_3$ solution. ↓ refers to the direction of water taken up by the material, ⇧ refers to the direction of the swelling.

network for water [20], and possibly for dissolved salts, thus increasing the permeability and decreasing the efficiency of bitumen as a semi-permeable membrane.

Two important remarks apply to this description. Firstly, the waste loading is an important parameter governing the swelling and soluble salts leaching. For waste loadings of ~50 wt% and higher, an increasing part of the mineral particles in the waste is no longer fully covered by a layer of bitumen, and the leaching of soluble salts such as $NaNO_3$ increases drastically (this is the so-called percolation effect [21,22]). It is likely that in such case the osmosis-induced swelling of the waste will be small to unexisting. Secondly, ageing by radiooxidation processes results in the hardening and embrittlement of bitumen [23–25]. This is expected to decrease the efficiency of bitumen as a semi-permeable membrane, and hence to result in a lower swelling degree and a higher $NaNO_3$ leaching. It can be noted here that the increase in the asphaltene fraction of the aged bitumen could have a positive effect on the radionuclide containment properties of the bitumen matrix [25].

The description of the water uptake, swelling, and $NaNO_3$ leaching processes as described above is valid for free swelling conditions. In geological disposal conditions free swelling will only be possible during a first phase, until the free volume in a 220 l drum is filled with swollen Eurobitum (assuming that this free volume will remain available during the whole free swelling phase). According to our calculations on the basis of results reported in [9,10], this could already be the case a few 100 years after contact with water. Once there is no more space for further swelling, the swelling Eurobitum will exercise an osmosis-induced pressure (see Appendix A), in first instance on the concrete secondary container, but finally on the surrounding clay formation. As a result, the surrounding clay will be slowly deformed, giving additional space for Eurobitum to swell. Due to its deformation, the counterpressure exerted by the clay will increase with the further swelling of the Eurobitum, *i.e.* a stress redistribution in the clay will occur. As long as the osmosis-induced pressure of the swelling Eurobitum can exceed the counterpressure exerted by the Boom Clay, swelling will go on. For characterisation and constitutive model development purposes, the tests that are reported in this paper are performed under different constant stress (oedometric) conditions, aiming at simulating various stages of the system evolution.

3. Experimental aspects

3.1. Non-radioactive reference Eurobitum and gamma irradiation

Non-radioactive reference Eurobitum was sampled from drum '0-2 CR15/16' that was produced during the 'cold runs (CR)' of EUROCHEMIC's bituminization installation in the 1970s (Table 1). The production method and composition of this non-radioactive reference Eurobitum are entirely similar to that of the radioactive Eurobitum, except for the presence of the radionuclides (less than 0.2 wt% in the real waste [1,2]).

Ring-shaped samples (inner diameter and height = 200 mm and 9–10 mm, respectively; outer diameter and height = 300 mm and 10–12 mm, respectively) of the non-radioactive reference Eurobitum were first gamma-irradiated in the absence of oxygen, to simulate the internal alpha–beta–gamma irradiation that a subsurface layer of the Eurobitum (*i.e.* a layer that is not contacted by water in the free swelling phase) experiences during interim storage and underground disposal until it comes in contact with water. Dose rates were higher than in the industrially produced radioactive Eurobitum, and varied between 150 Gy/h and 130 Gy/h, to deliver a total absorbed dose of ~750 kGy. Experimental details and results and discussion are given in [23,24]. Considering that for the hard (blown, oxidized) Mexpalt R85/40 the yield of radiolytically produced H_2 is about three times higher under alpha irradiation than under beta/gamma irradiation [2], we assume that the ageing effect of a dose of ~750 kGy corresponds to that of an alpha (~200 kGy) and beta–gamma (~100 kGy) dose absorbed after about 200 years. Scoping calculations indicated that for a disposal gallery in Boom Clay Eurobitum will come in contact with pore water within 100 years after closure of the disposal gallery [26].

3.2. Filling of the water uptake cell with gamma-irradiated Eurobitum

The laboratory tests to study the processes related to the water uptake by Eurobitum make use of water uptake cells that are placed in oedometers (Fig. 3).

The water uptake cells consist of three parts:

Table 1
Characteristics of the non-radioactive reference Eurobitum used in this study (data obtained from EUROCHEMIC/BELGOPROCESS).

Identification code	Wt% salts	Wt% $NaNO_3$[a]	Wt% H_2O	Density (g/ml)
0-2 CR15/16	38.9	28.5	0.39	1.31
Production date	Vol% salts	Vol% $NaNO_3$	Vol% other inorganic material	
11/01/1977	23	17	6	

[a] Destructive chemical and non-destructive Neutron Activation Analysis of subsamples from the drum, taken from the zone where the samples for the water uptake tests where sampled, indicate that the $NaNO_3$ content in this drum is rather ~31 wt%. On the basis of linear extrapolation, the density of the material would be rather 1.33 g/ml.

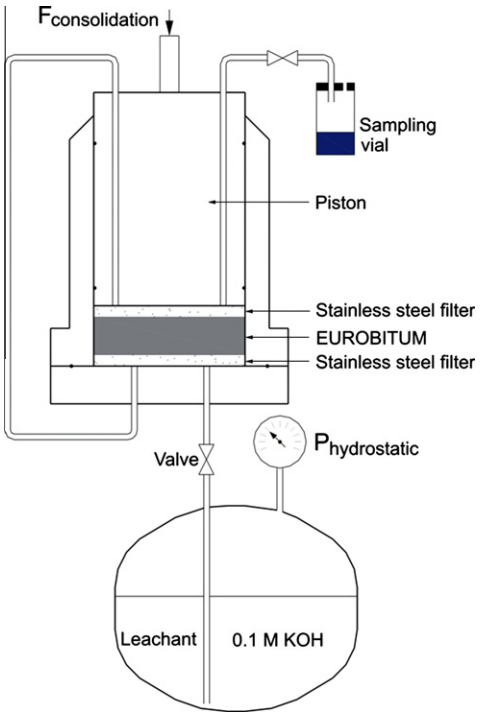

Fig. 3. Schematic visualization of the experimental set-up for water uptake tests with Eurobitum samples (diameter 38 mm, height 10 mm), contacted at both sides with 0.1 M KOH (SA/*V* = 0.32 or 0.45 mm^{-1}; see text) that is regularly sampled and renewed to maintain the water activity above 0.98. Note that the two solution compartments (for the two filters) are connected, assuring nearly the same water activity in both filters.

(i) a bottom plate with sintered stainless steel filter that supports the Eurobitum sample,
(ii) a movable piston with sintered stainless steel filter that contacts the upper surface of the Eurobitum sample, and
(iii) a 'holder' that is fixed with eight screws on the bottom plate, and that contains the filters, the Eurobitum sample, and the piston, so as to force the swelling of the Eurobitum sample in one (upwards) direction.

The average pore diameter of the sintered stainless filter is 3.2 μm, with a pore distribution range between 1.5 and 5 μm. Behind the filters, a 2 mm wide coiled channel that is connected with the small diameter ingoing and outgoing stainless steel tubes maximises the equilibration between the leached salts in the filter and the leachant. The holder is conceived in such a way that it also allows the cutting of the Eurobitum sample out of a larger sample without having to heat the sample. This avoids that the internal structure of the gamma-irradiated sample, which might influence the kinetics of the studied processes, is destroyed (*e.g.* the porosity caused by the radiolytic H_2 generation during the irradiation).

3.3. Loading–unloading test with the dry Eurobitum

After cutting the Eurobitum sample (38 mm diameter, variable height) out of a 50 mm diameter and 9–12 mm thick gamma-irradiated sample (Section 3.1), the piston with filter was introduced and the cell was placed in a front loader oedometer and submitted to two loading/unloading cycles. These loading/unloading steps allowed (i) to press the samples to a constant thickness of ~10 mm and to get a good contact between the sample on the one hand and the wall of the holder and the two filters on the other hand (first loading/unloading step), and (ii) to characterise the mechanical behavior of the bitumen samples (second loading/unloading step). The displacement of the piston was followed with a dilatometer (see below). For each loading step, an instantaneous volumetric deformation was followed by creep (*i.e.* a slow delayed deformation) [27,28]. For high stress levels ($\geqslant$2.2 MPa) volumetric creep deformations disappeared because the pore volume became negligible, and the material showed only a volumetric elastic response. However, under a high pressure, part of the bitumen or BW flowed into the pores of the sintered stainless steel filters and into the tiny void between piston and holder. This may have contributed to the observed creep.

The maximum stresses that were applied were 2.2, 3.3, or 4.4 MPa. These are the stresses that were to be applied during the subsequent water uptake tests. Values of 2.2 and 4.4 MPa are representative for respectively the hydrostatic pressure and the total pressure in the undisturbed Boom Clay at a depth of −220 m. Also during the second loading/unloading test, a continuous but slow negative displacement of the piston was observed, pointing to the flowing of bitumen in the filter pores and in the void between piston and holder. In total, eight stainless steel water uptake cells were prepared this way, labelled S0, S1, . . . , and S7.

3.4. Follow-up of swelling and $NaNO_3$ leaching

When the target stress of 2.2, 3.3, or 4.4 MPa on the BW samples was attained, 0.1 M KOH was introduced in the water circuit of the water uptake cell. A 0.1 M KOH solution was chosen to simulate to some extent so-called 'young cement water' – which is the first percolation water of concrete [29] – as in repository conditions the bituminous waste will be surrounded by cementitious materials. Young cement water contains a low $Ca(OH)_2$ concentration and high concentrations of NaOH and KOH, which are present as impurities in cement. To allow to monitor the leaching of Na^+, only KOH was used.

To assure that all air bubbles were removed, especially those in the edges and adsorbed on the filter material, the solution supply circuit was extensively and repeatedly rinsed with the 0.1 M KOH solution. Under normal operation conditions (*i.e.* no replacement of the leachant), the pressure on the 0.1 M KOH solution was maintained between 0.2 and 0.15 MPa (2 and 1.5 bar) absolute. It has to be noted that this liquid pressure is considerably lower than the hydrostatic pressure of 2.2 MPa prevailing in the Boom Clay at a depth of −220 m. As a result, the total effective stress on the sample, which is the difference between the total (vertical) stress and the liquid pressure, was close to the total stress. The SA/*V* ratio, this is the ratio of the geometrical external surface area of the Eurobitum sample that is in contact with the leachant and the leachant volume, was for five tests 0.45 mm^{-1} (surface: 22.7 cm^2; leachant volume: 5 cm^3). For three tests a pipette was included in the water supply circuit (not shown in Fig. 3), aimed at monitoring the uptake of solution by the sample. For these tests, the SA/*V* ratio was 0.32 mm^{-1} (~7 cm^3 of leachant).

The swelling of the samples in these constant stress tests was followed by measuring the displacement of the piston with a digital dilatometer that was connected to a data acquisition system that continuously measured the position of the piston. In general every 4–6 h, a measurement value was saved. Before the start of the experiments, each of the eight measurement chains was calibrated according to the ISO/IEC 17025 guidelines. The resolution of the dilatometers is 0.01 mm, the combined uncertainty on the displacement measurements is ~0.015 mm (95% confidence). Almost immediately after the injection of 0.1 M KOH, a clear positive displacement of the piston was observed. The small negative displacement due to the flowing of the BW in the filter pores and void between piston and holder is thus completely obscured by the swelling of the BW. The leaching of $NaNO_3$ was followed by replac-

ing the leachant with 10 cm^3 of fresh 0.1 M KOH solution at times $t = (2 \cdot x)^2$, with $x = 1, 2, 3, \ldots$, with t in days (*i.e.* sampling occurred 4, 16, 36, ... days after the start of the hydration). This sampling sequence was chosen because it is well-known that the uptake of water and the leaching of $NaNO_3$ from bituminized waste in free swelling conditions is reported to be a diffusion-controlled process [8–16]. The regular renewal of the leachant according to this sampling sequence was expected to enable to limit $NaNO_3$ concentration differences in the leachant. Measured $NaNO_3$ concentrations proved to vary between 0.05 and 0.3 M, thus maintaining the water activity of the leachant (0.1 M KOH + 0.05–0.3 M $NaNO_3$) above 0.98. At these high water activities, the water uptake rate is close to its maximal value [8,12], whilst meanwhile the tests are performed for a realistic, although somewhat low $NaNO_3$ concentration [26]. The sampling and renewal of the leachant had no measurable effect on the position of the piston. The sampled solutions were first weighed and recalculated to volume using a density of 1 g/ml, and then analyzed by Inductively Coupled Plasma Atomic Emission Spectroscopy (ICP-AES) and Ion Chromatography (IC), to measure the concentrations of Na^+ and Ca^{2+}, and nitrate and sulfate, respectively. Combination of the sampled volumes of leachant and the ion concentrations in the leachant allows to calculate the amount of $NaNO_3$ leached from the Eurobitum.

To demonstrate that osmosis is the key process governing the water uptake and swelling of Eurobitum BW, the 0.1 M KOH solution in one water uptake cell (cell S1) was replaced by a nearly saturated $NaNO_3$ solution (a saturated $NaNO_3$ solution was prepared at 15 °C, and then used at ~23 °C), ~1000 days after the start of the water uptake experiment. After ~1200 days, this nearly saturated $NaNO_3$ solution was replaced by a fresh nearly saturated $NaNO_3$ solution. During the contact with this solution, the leachant was not sampled. After ~1360 days, the nearly saturated solution was replaced by a fresh 0.1 M KOH solution. From that time onwards, the leachant was sampled monthly to quickly reach low $NaNO_3$ concentrations in the leachant.

3.5. End of the test – dismantling of the water uptake cells – analyses

Between ~800 and ~900 days after the start of the water uptake tests, three tests were stopped and dismantled. A fourth test was stopped after ~1500 days. To minimise the disturbance of the partially leached Eurobitum samples when retrieving the water uptake cells from the oedometers (removal of stress) and when pushing the samples out of the water uptake cell (high stress by means of a small press), the water uptake cells were first gently sprayed with liquid nitrogen until the Eurobitum samples were frozen. This procedure was first successfully tested on a water uptake cell containing a sample composed of an 8 mm thick partially leached sample that was sandwiched between two fully leached samples of 1 mm thickness. After retrieval, the frozen samples were first analyzed by micro-focus X-ray Computer Tomography (μCT). This analysis technique detects differences in attenuation of X-rays in the material, which are related to different densities, and hence allows to distinguish the leached and unleached zone. The resolution of this technique depends on the characteristics of the apparatus and on the distance between the sample and the detector (and thus on the size of the sample). The obtained μCT images have a voxel (volume element) size of about 94 μm, hence the resolution is 188 μm. Further details of the procedure and the interpretation of the results are given in [30].

Next, the samples were slowly heated to ambient temperature, and a razor blade was used to carefully separate the two filters from the sample. The sample itself was stored again at −20 °C immediately after removal of the filter. Probably because bitumen had flown into the filter pores, small and sometimes irregular parts of the outermost leached layers remained stuck on the filters and were thus withdrawn from the samples. The leached BW that remained stuck on the filters was carefully removed. Next, the filters were placed in a beaker with carbon tetrachloride (CCl_4) to dissolve the bitumen that during the test had penetrated in the filter pores. This washing procedure was repeated until all bitumen was leached from the filter. After evaporation of the CCl_4, the remaining bituminous phase was weighed to finally calculate the volume of bitumen that filled the pores of the filters.

Finally, the samples were frozen again before they were broken in two half-cylindrical parts by means of hammer and chisel. The central part of the fractured surface of one half-cylindrical part was then analyzed from top to bottom (*i.e.* from the utmost leached part at the upper filter to the utmost leached part at the lower filter) by Environmental Scanning Electron Microscopy (ESEM), to study the depth of water penetration and dissolution and leaching of $NaNO_3$. The resolution of this technique for our conditions was ~2 μm.

4. Results and discussion

4.1. Swelling of the BW samples

Fig. 4 shows the evolution of the displacement of the piston, *i.e.* the swelling, for the gamma-irradiated Eurobitum samples, under constant total stresses of 2.2, 3.3, or 4.4 MPa, when they are hydrated with 0.1 M KOH (and, for cell S1, with a nearly saturated $NaNO_3$ solution in the period 1019–1354 days and in a second period starting at 1670 days) under a solution pressure between 2 and 1.5 bar absolute, as a function of time. The swelling degree (expressed in percent) is calculated from these results as

$$\frac{(h-h_0)\times\pi\times r^2}{h_0\times\pi\times r^2}\times 100 = \frac{(h-h_0)}{h_0}\times 100 \qquad (1)$$

with h and h_0 the height of the swollen and the dry sample, respectively, and r the radius of the sample.

Several observations can be made. Firstly, it is seen that after more than 4 years of contact with 0.1 M KOH, all (remaining) samples continued to swell, with nearly no tendency to level off. For a water pressure of the leachant between 1.5 and 2 bar absolute, five of the eight samples swell(ed) at a rate of ~250 μm/year (~2.5 vol%/year, for both sides of the sample in contact with solution), independently of the applied stress. It should be stressed that

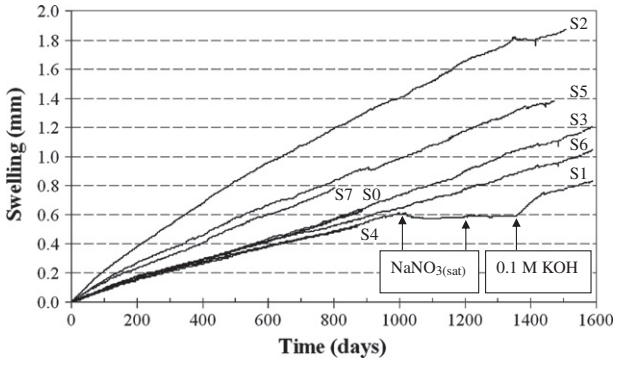

Fig. 4. Evolution of the (uni-axial) swelling of gamma-irradiated EUROBITUM samples at both sides in contact with 0.1 M KOH, which is regularly renewed to maintain the water activity above 0.98. The samples are allowed to swell against a constant stress of 2.2, 3.3, or 4.4 MPa (see Fig. 3). The uncertainty on the swelling measurements is 0.015 mm (95% confidence). From top to bottom: Cell S2 (2.2 MPa, +pipette (P)), S5 (4.4 MPa, +P), S7 (3.3 MPa, +P), S3 (4.4 MPa, −P), S0 (2.2 MPa, −P; note that the curve for this cell (stopped after 886 days) is mostly hidden behind the curve for S3); S6 (3.3 MPa, −P), S1 (2.2 MPa, −P), and S4 (4.4 MPa, −P; note that the curve for this cell (stopped after 872 days) is mostly hidden behind the curve for S1). These eight tests were not started at the same day.

Table 2
Summary of data on swelling of the BW samples in constant stress conditions.

Identification code	Duration (days)	Initial sample thickness (mm)[a]	Measured piston displacement (mm)	Equivalent height due to BW in filters (mm)	Corrected piston displacement (mm)	Volume increase (ml)[b]	Volume increase (%)
S0 (2.2 MPa, −P)	887	9.33	0.63	0.10	0.73	0.71–0.83	6.7–7.8
S4 (4.4 MPa, −P)	872	9.42	0.52	0.11	0.63	0.59–0.71	5.5–6.7
S5 (4.4 MPa, +P)	1472	9.33	1.40	0.09	1.49	1.59–1.69	15–16
S7 (3.3 MPa, +P)	805	9.83	0.78	0.15	0.93	0.89–1.05	8.0–9.5

[a] Based on μCT measurement, and including the contribution of BW in the filter.
[b] Calculated with respect to the measured and corrected piston displacement, respectively.

the measured swelling degrees are systematically smaller than the 'real' swelling degrees, due to the penetration of some BW into the filter pores. For the tests that were stopped after ~800–1472 days, the amount of bitumen or BW that thus did not contribute to the displacement of the piston – as determined by washing with CCl_4 – corresponded with a 'missed' piston displacement of ~0.09 to ~0.12 mm. In other words, if BW did not flow into the filter pores, the real swelling after this time would have been by up to 20% higher than the measured values. The total volume increases are summarized in Table 2. As it is not known when the BW was pressed into the filter pores (during the compressibility test, during the water uptake test, or both), the total volume increases were calculated on the basis of the piston displacement, either measured as such or corrected for the contribution of the BW in the filter pores. The values range from 0.6 to 1.7 ml (initial sample volume ~10.6 ml), or ~5 to ~16 vol%. These values are higher than the maximum volume increase due to the recrystallization of anhydrous calcium sulfate ('natural anhydrite'; density ~2.96 g/ml) to gypsum (density ~2.32 g/ml), which is only ~0.15 ml for a 10 mm thick sample. This is a clear indication that the swelling of bituminized salts is not only due to salts recrystallization, and that osmosis, involving the dissolution of dry $NaNO_3$ and the further dilution of the $NaNO_3$ solution, as well as the presence of a highly efficient semi-permeable membrane, strongly contributes to the swelling.

For three samples, S2 (2.2 MPa, +pipette (P)), S5 (4.4 MPa, +P), and S7 (3.3 MPa, +P), swelling rates of 350–550 μm/year (3.5–5.5 vol%/year) were measured. These higher swelling rates were observed for those systems for which the SA/V ratio is 0.32 mm^{-1}, that is, for which the water supply circuit includes also a pipette to follow the volume of water taken up by the Eurobitum. However, the slight difference in $NaNO_3$ concentration in the leachant due to the higher leachant volume and due to the slightly differing sampling procedure is too small to cause an effect on the swelling rate. This was among others confirmed by a test in nearly constant volume conditions where the leachant solution was not replaced during about 3 years (resulting in a $NaNO_3$ concentration of ~1 M instead of 0.05–0.3 M in the case of regular sampling), and where the regular renewal afterwards did not change the pressure increase rate [14]. In another constant pressure test, the pipette was closed from the system during several months during which no different swelling rates were observed. Therefore, it is more likely that the different swelling behavior is related to locally higher $NaNO_3$ contents in these samples, and/or to layers with a relatively higher content of smaller grains of $NaNO_3$.[3] This was evidenced by the results on $NaNO_3$ leaching, which are discussed in Section 4.2. A variation of the salt content and/or the grain size in the BW is quite normal, since the industrial bituminization process does not allow to produce perfectly homogeneous waste products. For this reason, all samples destined for water uptake tests are now systematically scanned by μCT, to check the homogeneity of the salts distribution.

A second important observation is that over the studied time period the swelling was not influenced by the counterpressure. This is clearly shown if the swelling degrees are plotted as a function of the counterpressure (Fig. 5; the three samples with a higher swelling degree, due to a higher $NaNO_3$ content (see Section 4.2), are not included in this figure). We believe that this is due to experimental counterpressures that are much smaller than the potential osmotic pressures in this system (see Appendix A). This is further discussed in Section 5.2.

Thirdly, it is seen that after a relatively short initial 'transition' stage, the swelling increased almost linearly with time, and not with the square root of time. At first sight, this is a somewhat surprising observation. On the basis of experimental results and mathematical approaches published in literature [8–12,15], we could expect the swelling to increase linearly with the square root of time, which is the normal behavior for a diffusion-controlled process such as the uptake of water by the BW. The results reported here, in combination with the insights obtained from the development of a constitutive law [27,28], suggest that in the constant stress conditions of our tests the ingress of water was not the (only) rate-limiting process, and that the swelling in these conditions is the overall result of several transient processes (diffusion, advection, dissolution, creep, involving a low permeability material with evolving thickness and properties) that moreover are non-linear and strongly coupled.

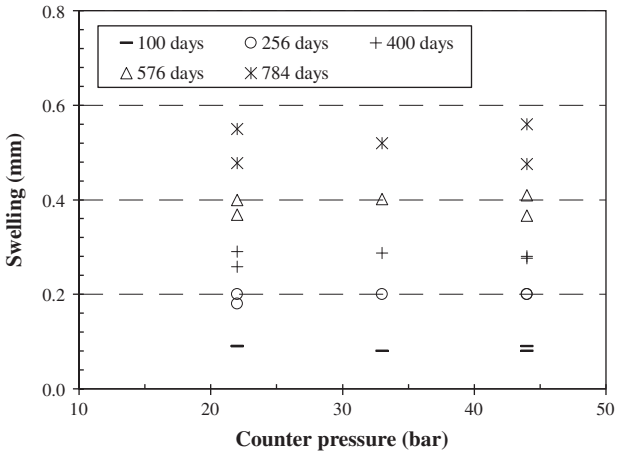

Fig. 5. Relation between swelling and counterpressure for the water uptake cells without pipette, with presumably the same $NaNO_3$ content in the samples (S0 (2.2 MPa or 22 bar), S1 (2.2 MPa), S3 (4.4 MPa or 44 bar), S4 (4.4 MPa), and S6 (3.3 MPa or 33 bar)). Beyond 784 days, two of the five tests were stopped, making it impossible to follow the evolution of the relationship for longer contact times.

[3] For an Eurobitum layer of 1 mm thick and 38 mm diameter, the $NaNO_3$ content is ~0.42 g (=28.5 wt%). If all of this $NaNO_3$ would be present as 1 μm diameter grains, such layer would contain 3.6×10^{11} grains of $NaNO_3$, and the thickness of the 'bituminous material' surrounding the $NaNO_3$ crystals (this is: the pure bitumen + sparingly soluble salts + (hydr)oxides of Fe, Zr, and Al; see Section 1) would be ~0.4 μm. If all of this $NaNO_3$ would be present as 10 μm diameter grains, the Eurobitum layer would contain 3.6×10^8 grains, and the thickness of the bituminous material around these grains would be ~4 μm.

For cell S1, it is seen in Fig. 4 that as a result of the replacement, after ~1000 days, of the 0.1 M KOH leachant by a nearly saturated $NaNO_3$ solution, the swelling rate fell down to almost zero. This is a clear demonstration that the water uptake and swelling of BW is to a large extent controlled by osmosis: since the water activity of the nearly saturated $NaNO_3$ solution was very close to the value of 0.74 for a saturated $NaNO_3$ solution or for dry $NaNO_3$, the difference of the water activity between the leachant and the saturated solution and dry $NaNO_3$ deeper in the BW sample became very small, and the water uptake process stopped. This also shows that the bitumen or bituminous material (as explained above) in these high counterpressure conditions continued to behave as a highly efficient semi-permeable membrane, even if it contained high amounts of non-bituminous material (~40 wt% or ~23 vol% of waste; see also Fig. 1 and Table 1). When examining the results in Fig. 4 in detail, it is seen that during the first ~50 days after the switch of the contact solution, a negative swelling, *i.e.* a contraction, occurred. This is due to the fact that immediately after the injection of the nearly saturated $NaNO_3$ solution the water activity gradient between filter and outer leached layer was switched from 'positive' (water flowing from the filter to the leached layer) to 'negative'. Because of this gradient switch, water moved from the low $NaNO_3$ concentration solution in the outermost layers of the leached BW (water activity ~0.98 or higher) to the high $NaNO_3$ concentration in the filter and tubings (water activity close to 0.74), whilst $NaNO_3$ diffused from the nearly saturated solution in the filter into the outermost BW layers, resulting in a negative swelling. With time, the $NaNO_3$ concentration in the filter and tubings increased again due to leaching from the sample, resulting in a zero water activity gradient, *i.e.* no more swelling or contraction. Replacement, after 1202 days, of the contacting solution with fresh nearly saturated $NaNO_3$ solution confirmed these findings: after a very short equilibration period due to the small but existing difference in water activity between the saturated $NaNO_3$ solution in the whole leached layer and the nearly saturated $NaNO_3$ solution in the filter and tubings, the water uptake process stopped again. When after ~1360 days the saturated $NaNO_3$ solution was replaced by 0.1 M KOH, the swelling rate increased, as expected for an osmosis-driven process. In a first phase the swelling rate increased faster than at the start of the water uptake test. This is attributed to the (relatively) higher permeability of the swollen and partially leached layer of the BW sample compared to the low permeability of dry BW, which, despite the presence of a re-compressed low permeability layer at the contact with the filters (see Sections 4.4 and 5), facilitates the ingress of water into the partially leached layer of the BW. When due to the ingress of water the $NaNO_3$ concentration profile in the leached layer was again similar to the one before the switch to a nearly saturated $NaNO_3$ concentration, the water uptake rate decreased to its value before the switch. Due to a short but significant temperature variation (~4 °C) and concomitant change of the swelling at ~1450 days – which is also visible for other the samples; note that the tests were not all started at the same day – the transition from a higher to a lower water uptake rate seems to be somewhat abrupt.

4.2. Leaching of $NaNO_3$

The bitumen (or the mixture of bitumen and sparingly soluble salts, (hydr)oxides, ...) surrounding the soluble salt crystals and the pores with salt solution is not a perfect semi-permeable membrane, and hence $NaNO_3$ (and other salts) can leach from the swelling BW. Fig. 6 shows the evolution of the cumulative amount of $NaNO_3$ that has leached out of the Eurobitum samples since the beginning of the experiments.

It is seen that just like the swelling the cumulative amount of leached $NaNO_3$ increased nearly linearly with time, in some cases

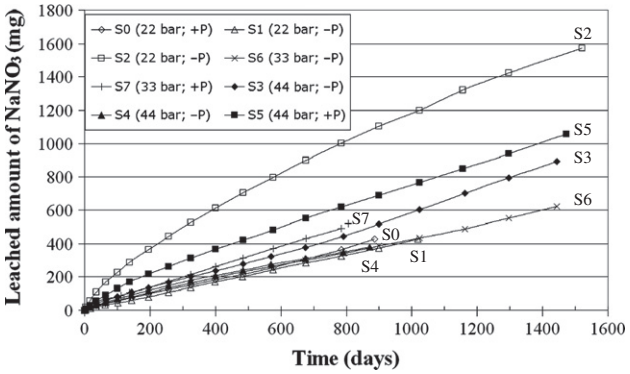

Fig. 6. Cumulative amount of $NaNO_3$ leached from the BW samples. The uncertainty on the cumulative leached amount of $NaNO_3$ is 10% (95% confidence).

after a short transition phase. As already discussed, this linear behavior is probably the combined result of different transient processes (diffusion, advection, dissolution, involving a low permeability material with evolving thickness and properties) that moreover are non-linear and strongly coupled. Since the sampling frequency was based on an expected diffusive behavior (see Section 3.4), the $NaNO_3$ concentration in the system between the different samplings (for which the duration between two consecutive sampling dates increased in the course of the experiment) was not constant but increased with the experiment running. Yet, in all cases the measured $NaNO_3$ concentrations varied between ~0.05 and ~0.3 M, corresponding with water activities of the leachate above 0.98, *i.e.* for which the effect on the water uptake and swelling rate is small [8,12].

The order of the curves for the cumulative amounts of leached $NaNO_3$ (Fig. 6) agrees well with that of the swelling, *i.e.* the higher the swelling, the higher the cumulative amount of leached $NaNO_3$ (Fig. 4). This agreement is shown graphically in Fig. 7. It is seen that the cumulative amount of leached $NaNO_3$ is linearly related to the swelling. This linear relationship is not unexpected. Whilst more water is taken up by the BW – either because the contact time with water increases (evolution with time) or because the BW contains layers with a locally higher $NaNO_3$ content and/or a different crystal grain size distribution, as for samples S2, S5, and S7 (see Footnote 3) – the BW continues to swell, and more $NaNO_3$ dissolves and leaches from the sample. The results for the three samples

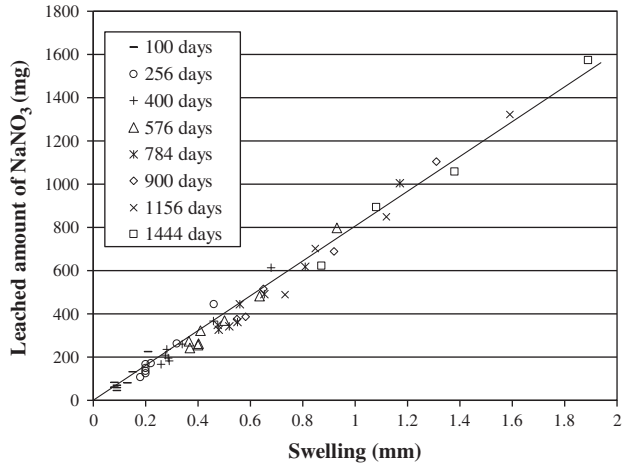

Fig. 7. Relation between the piston displacement (~swelling) and the cumulative amount of $NaNO_3$ leached out of the studied Eurobitum samples, for the water uptake tests without pipette shown in Figs. 4 and 6.

S2, S5, and S7 that show a higher swelling (Fig. 4) and a higher cumulative amount of leached $NaNO_3$ (Fig. 6) fit well with the results for the five samples that show a more 'similar' behavior. This corroborates our interpretation that the higher swelling observed for these samples is due to the higher $NaNO_3$ content and/or to the relatively higher amount of small size grains in these samples, or at least in the leached layers of these samples. It has to be noted that this linear relationship is only valid for samples with a waste loading of ~40 wt% and a $NaNO_3$ content of, say, ~25 to ~35 wt%. Especially at waste loadings $\gtrsim$ 50 wt% (*i.e.* the so-called percolation threshold [21,22]) the single mineral particles in the waste are no longer fully surrounded by a bitumen film. In such highly loaded BW, mineral clusters are present, which by the formation of interconnected pores severely increase the release rate of $NaNO_3$ and radionuclides, *i.e.* percolation effects. For such bituminized wastes, it is likely that the swelling – if any – and cumulative amount of leached $NaNO_3$ do not follow the linear relationship shown in Fig. 7.

In Fig. 7, for the five samples with similar swelling and $NaNO_3$ leaching behavior (S0, S1, S3, S4, S6; see Figs. 4 and 6), the upper points in the plot are related to the higher counterpressures (3.3 and 4.4 MPa), whereas the lower points in the graph are related to the lower counterpressures (2.2 and 3.3 MPa) (this is not shown in detail). Thus, in contrast to the (apparent) independence of the swelling on the counterpressure (Fig. 5), there seems to be for these five 'similar' samples a clear, yet small effect of the counterpressure on the cumulative leached amount of $NaNO_3$ This effect is visualized in Fig. 8. It is seen that a higher counterpressure resulted in a slightly higher cumulative leached amount of $NaNO_3$. A closer look at this figure indicates that this small difference was mainly created during the first ~250 days of the test, *i.e.* during the 'transition' period preceding the phase of (nearly) linear increase of the swelling (Fig. 4). The difference is possibly due to a larger $NaNO_3$ diffusion due to a slightly higher $NaNO_3$ concentration gradient for the systems at 4.4 MPa (see Section 5.2) and/or a higher amount of BW flown into the filter with subsequently a higher amount of easily leached $NaNO_3$.

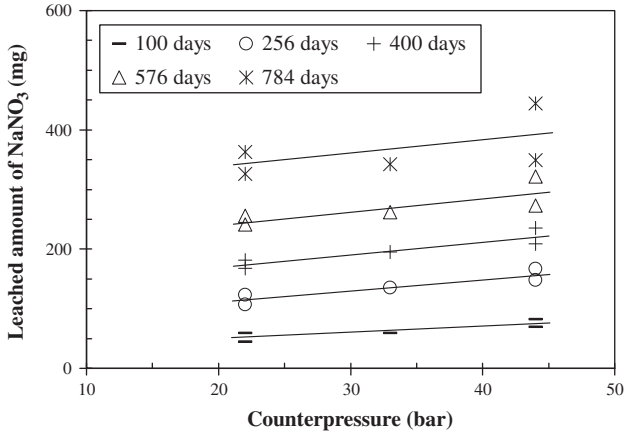

Fig. 8. Relation between the cumulative leached amount of $NaNO_3$ and the counterpressure for the water uptake cells without pipette, and with presumably the same $NaNO_3$ content (S0 (2.2 MPa or 22 bar), S1 (2.2 MPa), S3 (4.4 MPa or 44 bar), S4 (4.4 MPa), and S6 (3.3 MPa or 33 bar)).

Since the initial $NaNO_3$ content in the samples is ~4.2 g (28.5 wt%, Table 1), Fig. 6 shows that after 1500 days, for all samples but one ~15 to ~25 wt% of the initial $NaNO_3$ content had leached (Table 3; these percentages can be 10–15% lower for a 10–15% higher initial $NaNO_3$ content, see footnote in Table 1). For the sample S2 even ~35 wt% of the $NaNO_3$ content had leached in this period, but as already mentioned, the $NaNO_3$ content in this sample, or in the leached layer of this sample, was probably higher than ~4.2 g (28.5 wt%). Since $NaNO_3$ is a very soluble salt, these are rather low values. This confirms again that in restricted swelling conditions (*i.e.* counterpressure on the swelling material), bitumen behaves as a highly efficient semi-permeable membrane, even when containing a high amount of inorganic compounds. The amounts of leached $NaNO_3$ correspond with a (hypothetical) fully leached BW layer with a thickness of ~0.9 to ~2.4 mm for both sides, or ~0.45 to ~1.2 mm for one side (Table 3). We define the thickness of this fully leached layer as the equivalent leached thickness. According to this definition, the BW adjacent to this fully leached layer is completely dry and unleached, *i.e.* the $NaNO_3$ content equals the initial $NaNO_3$ content. It is obvious that in reality the salt content in the leached layers is higher than zero, and that hence the thickness of the 'leached layer' (or: the layer of BW that is affected by the ingress of water, *i.e.* from dry $NaNO_3$ with no molecules of water to a saturated or undersaturated $NaNO_3$ solution) is larger than this equivalent leached thickness. As will be shown further below, μCT and ESEM are very interesting tools to estimate the thickness of the leached layer.

4.3. μCT analysis of leached BW

The μCT images in Fig. 9 show the X-ray attenuation values in a slice perpendicular to the leachant surface of the Eurobitum BW samples of cell S0 (2.2 MPa, without pipette, 887 days) and S5 (4.4 MPa, with pipette, 1472 days). More μCT images can be found in [30]. The attenuation values are expressed as 16-bit integers (values between 0 and 2^{16}, *i.e.* values between 0 and 65,536). The full range of the colormap is used to visualize the attenuation values between 20,000 and 35,000 to improve the contrast in the μCT images and to better visualize the hydrated layers, as explained hereafter. The colour difference between both μCT images is due to the different tuning of the μCT apparatus for the two measurements. The apparent lower density in the centre of the sample in Fig. 9a is due to beam hardening, which is an artefact caused by the fact that the X-ray source of the μCT scanner emits polychromatic X-rays. The low energy X-rays of this spectrum are preferentially absorbed by the material, by which the effective energy of the beam increases as the beam penetrates deeper through the material. As a consequence, the outer part of an object seems to be denser than the inner part. Application of a hardware filter allows to decrease this effect, as seen in the right μCT image [30]. For clarity, the discussion below mostly relates to Fig. 9b, but the same comments – taking into account the remarks above –apply also to Fig. 9a.

Table 3
Summary of data on $NaNO_3$ leaching from the BW samples in constant stress conditions.

Code	Duration (days)	Cumulative amount of leached $NaNO_3$ (g)	% leached (for 28.5 wt% of $NaNO_3$ = 4.2 g per sample)	Equivalent leached thickness (two layers/one layer) for 28.5 wt% $NaNO_3$ (mm)
S0 (2.2 MPa, −P)	887	0.43	10.2	1.01/0.51
S4 (4.4 MPa, −P)	872	0.38	9.0	0.90/0.45
S5 (4.4 MPa, +P)	1472	1.06	25.2	2.42/1.21
S7 (3.3 MPa, +P)	805	0.52	12.4	1.23/0.61

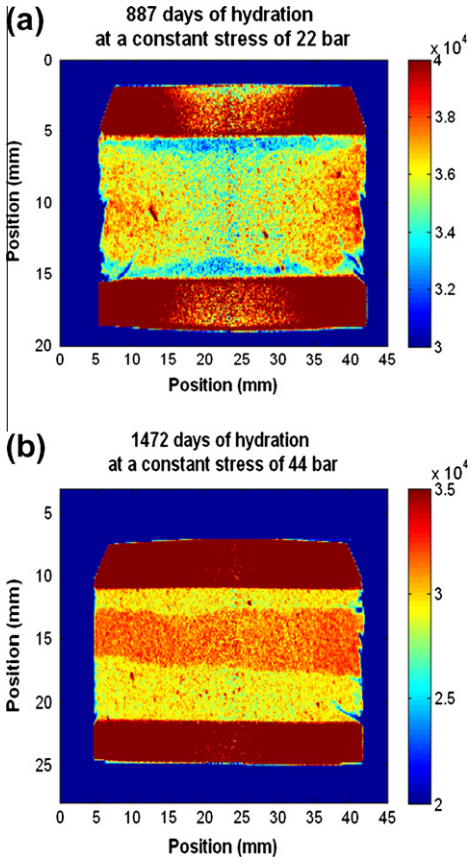

Fig. 9. μCT images: visualization of the hydration front in Eurobitum samples comprised between two stainless steel filters (shown in dark-red) with 28.5 wt% $NaNO_3$ after (a) 887 days of hydration under a constant stress of 2.2 MPa (22 bar; cell S0) and (b) 1472 days of hydration under a constant stress of 4.4 MPa (44 bar; cell S5). The attenuation values are expressed as 16-bit integers (range 20,000–35,000).

Several observations can be made. Firstly, the central part of the sample consists of a homogeneous mixture of denser and less dense substances. This is the dry Eurobitum. The main part of this layer is made up by (in orange-red represented) material consisting of very small size soluble and sparingly soluble salts (densities of the order of 2–3 g/ml) and (hydr)oxides of Fe, Zr, and Al (densities of 2–5 g/ml) that are intimately mixed with pure bitumen (density 1.03 g/ml). The more 'yellowish' spots are zones with a lower density, probably bitumen with less inorganic material. The few dark-red spots are probably due to locally higher contents of the waste constituents (soluble and sparingly soluble salts, (hydr)oxides of Fe, Zr, and Al, *etc.*). The central layer of dry Eurobitum is surrounded by two layers with a lower X-ray attenuation value (or: density). These are the (partially) leached layers. Also in these layers, isolated dark-red and orange-red spots can be seen, probably due to the locally higher contents of the waste constituents, where not all $NaNO_3$ has dissolved yet. In comparison with the dry Eurobitum, more yellow and even green zones are observed (Fig. 9b). The lower attenuation in these places is attributed to (i) the decreasing amount of dry $NaNO_3$ crystals (density of 2.26 g/ml) and (ii) the presence of pores filled with $NaNO_3$ solution (the density of a saturated and a 2 M $NaNO_3$ solution at 25 °C is respectively 1.39 and 1.10 g/ml [19]), of which in addition the diameter is larger then the diameter of the respective pores containing the dry $NaNO_3$ crystals (for instance, the volume increase upon full dissolution of a $NaNO_3$ crystal to a saturated $NaNO_3$ solution is a factor ~3.4). From the μCT images, it is further seen that the thickness of these partially leached layers is not constant over the sample diameter. This is possibly related to the fact that due to the high pressures in these systems some bitumen and/or BW is pressed into the pores of the stainless steel filters, resulting in an extra diffusion limitation for water ingress and salts leaching. Following this idea, the regions with a thinner leached layer would be in contact with a filter zone with more bitumen and/or BW in the pores [30]. The differing thickness of the leached layers may also be caused by differences in $NaNO_3$ content and crystal size distribution (see Footnote 3). This is very likely also the reason for the observation for sample S5, where the lower leached layer is almost two times thicker than the upper leached layer (Fig. 9b), and for which a higher swelling and cumulative amount of leached $NaNO_3$ was observed (Figs. 4 and 6).

Furthermore, the overall density of both leached layers is very similar and, at least at first sight, constant over the whole thickness of these layers. The transition between the dry Eurobitum and the leached layers is quite sharp: a few hundred μm. The total average thickness of the leached layers as determined from the μCT images is ~2.5 mm (Fig. 9a; cell S0, 887 days at 2.2 MPa) and ~6.2 mm (Fig. 9b; cell S5, 1472 days at 4.4 MPa). The 'μCT' thicknesses of the leached layers of all analyzed samples are summarized in Table 4. They are systematically higher, by a factor of 2.6–2.9, than the total equivalent leached thickness defined in the previous section. This shows, as expected, that the evolution of the $NaNO_3$ content (not the dissolved $NaNO_3$ concentration!) in the leached samples does not change abruptly from zero to its maximum value, *i.e.* no congruent $NaNO_3$ dissolution and leaching.

Despite the apparently constant density of the leached layer, a closer look at the evolution of the average attenuation in one (vertical) slice, with thickness equal to the voxel size of 94 μm, reveals that there are attenuation gradients over the leached layer (slices ~200 to ~225) (Fig. 10). The gradient between slices 200 and ~208 is related to the fact that each slice in this layer contains both non-hydrated BW and hydrated BW. The closer to the non-hydrated BW part (*i.e.* closer to slice 200), the more non-hydrated high-density zones are present in the slices, resulting in a higher mean attenuation value. The gradient in mean attenuation value between slices ~208 and ~218 is probably related to a gradient in salt content over the leached layer, and not or much less to a gradient in $NaNO_3$ concentration in the pore solution, for two reasons:

(1) As already explained, the dissolution of salts results in a larger decrease in density (namely from 2.26 g/ml for dry $NaNO_3$ to 1.39 g/ml for a saturated $NaNO_3$ solution at 25 °C) than a dilution of the salt solution (*e.g.* 1.10 g/ml for a 2 M $NaNO_3$ solution at 25 °C).

Table 4
Summary of data on the thickness of the leached layer.

Code	Duration (days)	Equivalent leached thickness (two layers / one layer) for 28.5 wt% $NaNO_3$ (mm)	Leached thickness based on μCT (mm)[a]	Ratio	Leached thickness based on ESEM (mm)	Ratio
S0 (2.2 MPa, −P)	887	1.01/0.51	2.65	2.6	5.30	5.2
S4 (4.4 MPa, −P)	872	0.90/0.45	2.34	2.6	5.31	5.9
S5 (4.4 MPa, +P)	1472	2.42/1.21	6.29	2.6	7.09	2.9
S7 (3.3 MPa, +P)	805	1.23/0.61	3.53	2.9	3.55	2.9

[a] Corrected for the amount of BW in the pores of the two filters.

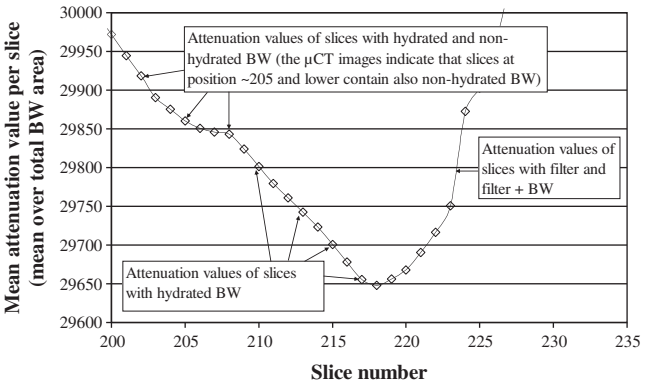

Fig. 10. Plot of the mean attenuation value per slice parallel to the sample surface in function of the position in the bottom leached layer of sample S5, showing a small attenuation gradient over the leached layer. The thickness of each slice equals 1 voxel size (94 μm). The attenuation values are expressed as 16-bit integers (range 20,000–35,000).

(2) In addition, as will be discussed in Section 5.2, the (average) $NaNO_3$ concentration is probably very high over the whole leached layer, except near the outer surfaces.

4.4. ESEM analysis of leached BW

Whereas μCT gives an overall but less detailed view of the leached sample, ESEM of the surface of the cleaved sample (Fig. 11a) yields detailed information on the porosity of a very thin band (~0.6 mm width), including the transition layer between the dry and the leached part. In Fig. 11b and c two ESEM images of the fracture surface of sample S0 are shown. Similar images were obtained for sample S5 and for other samples [30]. Some of the first ESEM analyses were seriously hindered by the adsorption of water vapour by the hygroscopic $NaNO_3$ and the subsequent dissolution (deliquescence, [6,32]), resulting in the appearance – even during the ESEM analysis – of an irregularly shaped 'paste' covering parts of the sample. The use of silicagel during the transport of the samples proved to help to avoid this problem. Typically 30 images were to be taken per sample to map the whole thickness of the ruptured surface, *i.e.* from the upper leached layer (in contact with the filter on the piston) to the lower leached layer (in contact with the filter on the base plate).

The image in Fig. 11b was obtained at the upper outer layer. It has to be noted that for most samples, due to the strong sticking of the swollen sample onto the filters (under a pressure of 2.2–4.4 MPa), (parts of) the outermost leached layers remained stuck on the filters, and could therefore not be scanned. The image in Fig. 11c was taken at the centre of the sample. There is a clear difference between these two images. In the leached layer (Fig. 11b), distinct pores, with a pore diameter varying between ~3 and ~30 μm could be seen over nearly the whole scanned surface. The same observations could be made for the many other ESEM images of the leached layers of this and other samples, irrespective of the counterpressure. It was not possible to distinguish any significant difference of the average pore size and the pore size distribution for the four studied samples. At the outermost edge of the sample, which was in contact with the filter, a very thin layer (<100 μm) with very low porosity was observed (Fig. 11b). This low permeability layer is believed to be formed by the compression of the outermost leached layer of the sample by the $NaNO_3$ leaching from this layer in combination with the osmotically-driven transport of water deeper into the sample, and this under the high stress on the sample. In contrast to the leached layer, almost no pores can be seen on the dry part of the sample (Fig. 11c). It is not clear whether the few small pores that can be seen in this image are air-filled pores or $NaNO_3$ solution containing pores. These latter may locally have formed due to rapid water ingress through small fissures in the sample and/or along the preferential pathways formed by the insoluble but hydrophylic salts and (hydr)oxides [20]. At the scanned surface of the samples, especially at the level of the 'dry' material, but also at the level of the leached layer, crystalline material can be observed, which according to the morphology is $NaNO_3$. EDX measurements confirm that these crystals mainly consist of $NaNO_3$, with traces of Ca and S, pointing to the presence of $CaSO_4$. Thus also in the leached layer undissolved $NaNO_3$ crystals are still present.

By compiling the 30 ESEM images per sample into one picture – of which the ratio of height and width is too large to include this picture in this paper – it is possible to have a very local view of the whole sample thickness, enabling to determine the local thickness of the leached layer, including the transition layer between dry Eurobitum and the bulk of the leached layer (cfr. Fig. 10). The values of the thickness are also included in Table 4. Considering that for many samples the thickness of the leached layers was not constant over the whole sample – as revealed by the μCT analysis (Fig. 9) – the 'local' thickness of the leached layers as

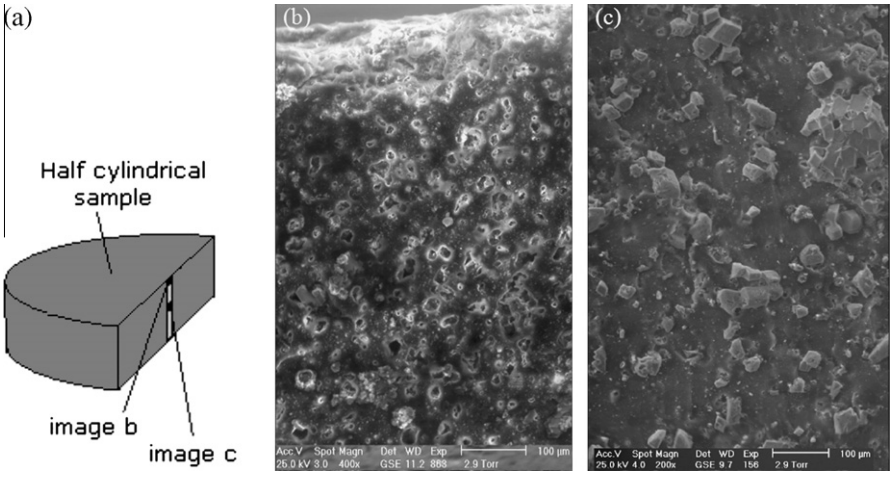

Fig. 11. ESEM images of the fracture surface of Eurobitum sample S0, after 887 days of hydration. (a) Visualization of the positions where the ESEM images were recorded. (b) ESEM image of a small area near the sample surface that has been in contact with the leachant solution. (c) ESEM images of a small area in the middle of the sample.

determined from the ESEM analysis corresponds mostly well with the average thickness as determined by μCT.

5. General discussion and conclusions

In this paper, the swelling of and $NaNO_3$ leaching from cylindrical non-radioactive Eurobitum bituminized waste samples due to the uptake of water, has been studied in constant stress (or: constant counterpressure; range: 2.2–4.4 MPa) conditions for periods up to about 4 years. During the study, four tests were stopped and the leached samples have been analyzed by micro-focus X-ray Computer Tomography (μCT) and Environmental Scanning Electron Microscopy (ESEM). The complete set of data enables a consistent interpretation of the observations and leads to an improved understanding of the phenomenology of the water uptake, swelling, and $NaNO_3$ leaching in restricted swelling conditions.

5.1. Main processes

The results and observations reported in this paper show that the uptake of water by, and the subsequent swelling of bituminized waste with a waste loading of ~40 wt% and containing ~28 wt% of soluble salts ($NaNO_3$), are largely controlled by osmosis. Indeed, after about 4 years of contact with water (0.1 mol/L KOH), the swelling varied between ~10% and 20%, which is higher than can be explained by recrystallization of the 4–6 wt% of sparingly soluble $CaSO_4$. In addition, the evolution of the swelling when changing the $NaNO_3$ concentration in the contacting solution followed the expected behavior of a system controlled by osmosis. The bitumen surrounding the soluble salts and other inorganic compounds proves to behave as a very efficient semi-permeable membrane, especially when submitted to a sufficiently high counterpressure (*i.e.* swelling in (semi-)confined conditions). The diffusion of $NaNO_3$ out of the BW combined with the external stress and the osmosis-driven transport of water from the outermost pores with a lower $NaNO_3$ concentration (higher water activity) towards deeper pores with a higher $NaNO_3$ concentration (lower water activity), contribute to a local consolidation and the formation of a re-compressed, low porosity layer at both contact sides with the filter. The re-compressed layers in turn contribute to the low permeability of the whole material, and hence to the importance of osmosis as the main process governing the swelling of BW. The fact that after a relatively short initial 'transition' stage the swelling increased almost linearly with time, and not with the square root of time, suggests that in the constant stress conditions in our tests the ingress of water was not the (only) rate-limiting process, and that the observed swelling and swelling rate are the overall result of several transient processes (dissolution, diffusion, advection, creep, involving a low permeability material with evolving thickness and properties) that moreover are non-linear and strongly coupled.

5.2. Average $NaNO_3$ concentration in the leached layer

Combination of the data on swelling (Section 4.1), cumulative amount of leached $NaNO_3$ (Section 4.2), thickness of the leached layer as obtained from μCT and ESEM (Sections 4.3 and 4.4), initial $NaNO_3$ content in the dry Eurobitum, and density of $NaNO_3$ and dry Eurobitum, allows to calculate the average $NaNO_3$ concentration in the leached layer. For the samples S0 and S5 (Fig. 9), the calculated values are 3.8 ± 3.8 M and 3.9 ± 3.9 M, respectively. For the four samples that were already stopped and analyzed, the average $NaNO_3$ concentration in the leached layer is 4.2 ± 4.2 M (95% confidence interval) (Table 5). It has to be noted that these values are to be reduced by some 10% to 20% to take into account that not all $NaNO_3$ crystals in the leached layers are dissolved (this fraction can only be roughly estimated, as it is nearly impossible to measure it). The uncertainty on the average $NaNO_3$ concentration in the leached layer is very high, and is due to the large uncertainties on the sample thickness and the thickness of the leached layers at the end of the water uptake experiment, as obtained from the μCT images (Fig. 9a and b), and the uncertainty on the total leached amount of $NaNO_3$ at the end of the water uptake experiment (the effect of the uncertainty on the $NaNO_3$ content of the sample is not included, but is relatively small).

The fact that according to the ESEM images the leached layers still contain 'solid' $NaNO_3$ might suggest that the $NaNO_3$ concentration in the pores with dissolved $NaNO_3$ is close to saturation (7.85 M). This is considerably higher, yet not always statistically significantly different, than the calculated average concentrations. It is possible that the bitumen surrounding the undissolved $NaNO_3$ crystals is locally thicker and/or contains no or less sparingly soluble salts and (hydr)oxides, so that water diffuses extremely slowly towards these crystals. According to this idea, 'islands' with dry, undissolved $NaNO_3$ would exist along with pores containing dissolved $NaNO_3$, of which the $NaNO_3$ concentration may vary between saturation and ~1 M (for a counterpressure of 4.4 MPa) or ~0.5 M (for a counterpressure of 2.2 MPa; see Table A.1). The $NaNO_3$ that is leached from the BW probably comes from both the nearby and the deeper layers. We have too little insight on the relative contribution of both zones, but the fairly equal distribution of undissolved $NaNO_3$ grains over the whole leached layer suggests that dissolved $NaNO_3$ also diffuses from the deeper layers to the outer layers. Whatever the exact mechanism, the high and probably nearly constant average $NaNO_3$ concentration throughout the leached layer is remarkable. It is likely the combined result of (i) the continuous transfer of water deeper into the sample, (ii) the continuous transfer of $NaNO_3$ from both deeper inside the sample (water hydration front) and from partly dissolved $NaNO_3$ ('islands') and $NaNO_3$ solution filled pores in the leached layer, towards the filters, and (iii) the presence of a thin re-compressed layer of leached bitumen that, in addition to the bitumen surrounding the $NaNO_3$ solution containing pores, behaves as a low permeable and highly efficient semi-permeable membrane.

The values in Table 5 are average concentrations, which are believed to be quite constant over the major part of the leached layer. It is possible that a small concentration gradient exists, with a higher $NaNO_3$ concentration closer to the dry Eurobitum, and a lower $NaNO_3$ concentration closer to the outer layer, but this hypothesis cannot be ascertained by analytical results. In any case, the high average dissolved $NaNO_3$ concentration in most of the leached (or: leaching) layer results in a high (average) osmotic pressure (Appendix A and Table A.1), which is considerably higher than the counterpressures in the test. Only in a very thin layer close to the filter, and insofar as the surrounding bitumen or bituminous material in this layer still behaves as a highly efficient semi-permeable membrane, $NaNO_3$ solution concentrations might be different for the different counterpressures, with a higher $NaNO_3$ concentration, and hence a lower dilution (or: swelling), for the higher counterpressure (Table A.1; ~1 mol/L at 4.4 MPa and ~0.5 mol/L at 2.2 MPa). This, in combination with at least

Table 5
Average $NaNO_3$ concentration in the leached layers of the four dismantled samples.

Code	Duration (days)	Average $NaNO_3$ concentration (mol/L)
S0 (2.2 MPa, −P)	887	3.8 ± 3.8
S4 (4.4 MPa, −P)	872	3.9 ± 3.9
S5 (4.4 MPa, +P)	1472	4.4 ± 4.4
S7 (3.3 MPa, +P)	805	4.4 ± 4.4
Average		4.2 ± 4.2

two sources of variability (local variability of the $NaNO_3$ content and related pore size distribution; bitumen or bituminous material behaving locally more or less as a highly efficient semi-permeable membrane) and the small difference in pore size for a twofold dilution, explains why there is no measurable effect of the counterpressure on the swelling, at least not in the range of counterpressures applied in this study.

5.3. Phenomenology of the swelling in restricted swelling conditions and expected evolution of the system

From the above, it is concluded that the phenomenology of the water uptake, swelling, and salts leaching in restricted swelling conditions differs considerably from what is observed for the free swelling (Fig. 2), where a steady increase of the pore size is observed, for which a steady decrease of the $NaNO_3$ concentration is postulated [8,11,12]. Fig. 12 presents schematically the phenomenology of the water uptake and swelling in restricted swelling (constant stress) conditions for a binary mixture of bitumen and $NaNO_3$.

We intend to continue to monitor some of the remaining water uptake tests until the swelling stops. Based on the data reported in this work, it can be expected that it will take still several years before the hydration front has reached the centre of the samples in the remaining water uptake tests, and it will require even more time before all $NaNO_3$ has dissolved. During some part of this time the samples will continue to swell. We can only speculate about when and how the swelling will finally stop. We expect that at some point in time a further volume increase due to the water uptake by the dry $NaNO_3$ crystals and/or the dilution of the concentrated $NaNO_3$ solutions in the pores will be increasingly more compensated by a re-compression of the leached layer, causing the swelling to level off before dissolution of all $NaNO_3$ and/or advanced dilution of the concentrated $NaNO_3$ solution. Finally, when all $NaNO_3$ will be dissolved and the average $NaNO_3$ concentration in the BW will start to decrease, the related osmotic pressure will decrease accordingly, and eventually nearly full re-compression of the leached BW is expected to occur. Depending on the osmotic efficiency of the re-compressed material, this may take a very long time. A similar phenomenology is anticipated for a full-scale drum with Eurobitum, yet with different kinetics, a.o. because of the effect of ageing of the bitumen [23–25]. From a safety point of view, it is important to know at which swelling degrees the BW will stop to swell, as this determines the maximum volumetric deformation of the host formation (this latter depends also on the stress–strain relationship (constitutive model) of the host clay, which is also a subject of ongoing research). It can be noted here that for bituminized waste with a waste loading of ~50 wt% or higher (*i.e.* the percolation threshold [21,22]) the formation of a thick re-compressed leached layer might result in the osmosis-induced swelling of the remainder of such bituminized waste product.

The observations reported in this paper (swelling, $NaNO_3$ leaching, linear increase of the swelling and $NaNO_3$ leaching with time, absence of an important effect of the counterpressure on the swelling in the studied range (2.2–4.4 MPa), formation and growth of a low porosity – low permeability outer layer) can be reproduced well with the fully coupled chemo-hydro-mechanical constitutive model for Eurobitum, developed by the International Centre for Numerical Methods and Engineering (CIMNE – Polytechnical University of Cataluña, Barcelona, Spain), and many results are presented in [18]. For this model the balance equations for water, dissolved salts, crystals and solid phase were written with taking into account the coupled flows, namely osmotic flow and ultrafiltration, and the dissolution/precipitation of salts. The balance equations are coupled to the equilibrium of stresses, and the formulation has been included as an extension in a coupled thermo-hydro-mechanical program (code Bright®).

An important objective of the ongoing research program is to be able to make sound predictions regarding the interaction between the swelling Eurobitum and the surrounding Boom Clay, to support the decision about the number of waste drums that can be placed per meter of gallery without risking an unacceptably high deformation and hence perturbation of the host formation. The improved understanding of the phenomenology of the water uptake, swelling, and $NaNO_3$ leaching in restricted swelling conditions, integrated in the fully coupled CHM constitutive model, offers good perspectives to achieve this goal.

Acknowledgements

This work is undertaken in close co-operation with, and with the financial support of ONDRAF/NIRAS, the Belgian Agency for the Management of Radioactive Waste and Enriched Fissile

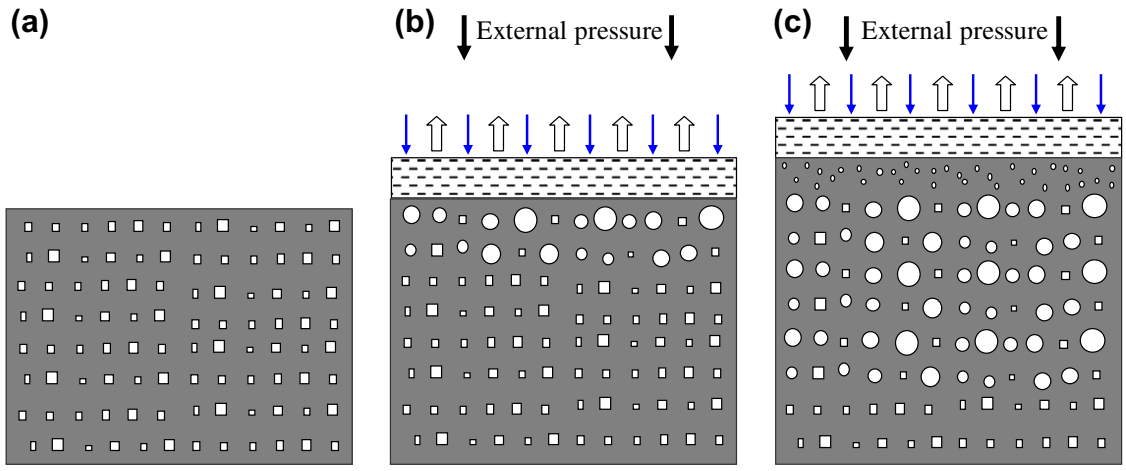

Fig. 12. Simplified schematic representation of the water uptake and swelling in a binary bitumen – $NaNO_3$ mixture in constant stress (restricted) swelling conditions. (a) Dry mixture of bitumen and $NaNO_3$ crystals. (b) Mixture in which in the first layers most of the $NaNO_3$ crystals are partially or completely dissolved (to an oversaturated, saturated, or undersaturated solution). (c) Mixture such as in (b), but with a re-compressed low permeable layer. □ = dry $NaNO_3$ crystal, ○ = pore with $NaNO_3$ solution, ▭ = filter (and, not drawn, piston) at a given counterpressure. ↓ refers to the direction of water taken up by the material, ⇧ refers to the direction of the swelling.

Materials, as part of its programme on geological disposal of medium-level long-lived waste.

The suggestions by and the discussions with Maarten Van Geet (ONDRAF/NIRAS) and Geert Volckaert (SCK·CEN), and the technical assistance of Patrick Boven, Jef Peeters, and Wim Verwimp (SCK·CEN), are greatly appreciated.

Appendix A

The osmotic pressure Π can be considered as the pressure that needs to be exerted on a solution to prevent osmosis-driven flow of solvent into that solution when it is separated from the pure solvent by a semi-permeable membrane. Conversely, it can be considered as the pressure that is exerted by such solution when osmosis-driven flow of solvent, and related volume increase, is made impossible (*i.e.* constant volume). The osmotic pressure can be calculated on the basis of the following equation [31]:

$$\Pi = \frac{R \cdot T}{v_{H_2O}} \cdot \ln\left(\frac{p^0_{H_2O}}{p_{H_2O}}\right) \quad (2)$$

in which R is the ideal gas constant (0.0821 L atm/K mol or 8.314 J/K mol), T the temperature (K; 25 °C = 298.15 K), v_{H_2O} the partial molar volume of water (L/mol), $p^0_{H_2O}$ the water vapour pressure of pure water and p_{H_2O} the water vapour pressure above the salt solution (*e.g.* mm). The ratio of p_{H_2O} and $p^0_{H_2O}$ is the water activity. For a saturated $NaNO_3$ solution at 25 °C (7.8457 mol/L), the water activity equals 0.74 [19], and the corresponding osmotic pressure is as high as 422 atm (428 bar or 43 MPa). The osmotic pressure decreases with increasing water activity (or: decreasing $NaNO_3$ concentration). For a given amount of $NaNO_3$ surrounded by a semi-permeable membrane that can stretch whilst maintaining its membrane properties, a lower $NaNO_3$ concentration means a higher degree of dilution, hence a higher degree of swelling. Table A.1 gives the osmotic pressures calculated according to Eq. (2) for the water vapour pressures measured by Pearce and Hopson [19], as well as some specific values that were calculated after fitting the osmotic pressure – $NaNO_3$ solution concentration relationship of the primary data in the table.

Table A.1
Water vapour pressure (mm Hg), water activity, and osmotic pressure (MPa) calculated for different $NaNO_3$ solution concentrations (mol/L) at 25 °C [19,31].

$NaNO_3$ concentration (mol/L)	Water vapour pressure (mm Hg)	Water activity	Osmotic pressure (MPa)
Osmotic pressures calculated with Eq. (2) using the data of Pearce and Hopson [19]			
7.85	17.554	0.739	42.8
7.41	17.957	0.756	39.6
6.86	18.448	0.777	35.7
6.27	18.987	0.799	31.6
5.65	19.484	0.820	27.9
4.99	19.999	0.842	24.2
4.28	20.534	0.865	20.5
3.53	21.092	0.888	16.7
2.73	21.691	0.913	12.7
2.31	21.998	0.926	10.7
1.88	22.332	0.940	8.6
1.43	22.650	0.954	6.6
0.97	23.006	0.969	4.4
0.78	23.152	0.975	3.5
0.59	23.299	0.981	2.7
0.39	23.446	0.987	1.8
0.20	23.596	0.993	0.9
0.10	23.674	0.997	0.5
0.00	23.752	1.000	0.0
Osmotic pressures calculated with $Y = 0.654 \cdot x^2 + 44.758 \cdot x$ ($R^2 = 1$), with $x = NaNO_3$ solution concentration (mol/L), obtained by fitting part of the above data (range 0–3.53 mol/L) with a second order polynomial			
0.97	Not calculated	Not calculated	4.4
0.73	Not calculated	Not calculated	3.3
0.49	Not calculated	Not calculated	2.2

References

[1] CEC 1989, Handbook of reference medium active waste (RMA), EUR 12482, first ed., European Commission, Luxembourg, 1989.
[2] E. Valcke, A. Sneyers, P. Van Iseghem, The long-term behavior of bituminized waste in a deep clay formation, in: Proc. of Safewaste Conf., October 1–5, 2000, vol. 2, Montpellier, France, 2000, pp. 562–573. <www.sfen.fr>.
[3] ONDRAF/NIRAS, The Long-term Safety Assessment Methodology for the Geological Disposal of Radioactive Waste, ONDRAF/NIRAS Report NIROND TR-2009-14 E, 2009. <www.nirond.be>.
[4] M. De Craen, L. Wang, M. Van Geet, H. Moors, Geochemistry of Boom Clay Pore Water at the Mol Site, Scientific Report SCK·CEN-BLG-990, SCK·CEN, Mol, Belgium, 2004. <www.sckcen.be>.
[5] E. Valcke, A. Mariën, M. Van Geet, Mater. Res. Soc. Symp. Proc. 1193 (2009) 105–116.
[6] S. Carroll, L. Craig, T.J. Wolery, Geochim. Trans. 6 (2005) 19–30.
[7] P. Morgan, A. Mulder, The Shell Bitumen Industrial Handbook, Shell Bitumen, 1995.
[8] J. Sercombe, B. Gwinner, C. Tiffreau, B. Simondi-Teisseire, F. Adenot, J. Nucl. Mater. 349 (2006) 96–106.
[9] A. Sneyers, P. Van Iseghem, Mater. Res. Soc. Symp. Proc. 506 (1998) 565–572.
[10] K. Brödersen, G. Brunel, R. Gens, F. Lambert, J.C. Nominé, A. Sneyers, P. Van Iseghem, Characteristics of Bituminized Radioactive Waste, Final Report for Contract No. FI2W-CT-91-0025, EUR 18228 EN, Luxembourg, 1998.
[11] B. Simondi-Teisseire, S. Camaro, P.P. Vistoli, V. Blanc, M.A. Romero, Long-term behavior of bituminized waste in presence of water, in: Proc. of Safewaste Conf., October 1–5, 2000, vol. 2, Montpellier, France, 2000, pp. 574–581. <www.sfen.fr>.
[12] B. Gwinner, J. Sercombe, C. Tiffreau, B. Simondi-Teisseire, I. Felines, F. Adenot, J. Nucl. Mater. 349 (2006) 107–118.
[13] I.A. Sobolev, A.S. Barinov, M.I. Ojovan, N.V. Ojovan, I.V. Startceva, Z.I. Golubeva, Mater. Res. Soc. Symp. Proc. 608 (2000) 571–576.
[14] A. Mariën, S. Smets, X. Li, E. Valcke, Mater. Res. Soc. Symp. Proc. 1107 (2008) 151–159.
[15] X. Lefebvre, J. Sercombe, A. Ledieu, B. Gwinner, F. Adenot, Mater. Res. Soc. Symp. Proc. 932 (2006) 681–688.
[16] A. Mariën, S. Smets, E. Valcke, Mater. Res. Soc. Symp. Proc. 1193 (2009) 513–520.
[17] X. Li, F. Bernier, E. Valcke, Mater. Res. Soc. Symp. Proc. 932 (2006) 751–758.
[18] N. Mokni, S. Olivella, E. Valcke, A. Marien, S. Smets, X. Li, Deformation and flow driven by osmotic processes in porous materials: application to bituminized waste materials, Transport in Porous Media, in press, doi:10.1007/s11242-010-9644-2.
[19] J.N. Pearce, H. Hopson, J. Phys. Chem. 41 (1937) 535–538.
[20] S. Le Feunteun, O. Diat, A. Guillermo, A. Ledieu, A. Poulesquen, Mater. Res. Symp. Proc. 1193 (2009) 505–512.
[21] A.S. Barinov, M.I. Ozhovan, I.A. Sobolev, Soviet Atomic Energy 65 (6) (1988) 403–405.
[22] M.I. Ojovan, W.E. Lee, An Introduction to Nuclear Waste Immobilisation, Elsevier, Amsterdam, 2005. 315 p.
[23] F. Rorif, E. Valcke, P. Boven, H. Ooms, J. Peeters, S. Smets, Mater. Res. Soc. Symp. Proc. 932 (2006) 689–696.
[24] E. Valcke, F. Rorif, S. Smets, J. Nucl. Mater. 393 (2009) 175–185.
[25] M.I. Ojovan, N.V. Ojovan, Z.I. Golubeva, I.V. Startceva, A.S. Barinov, Mater. Res. Soc. Symp. Proc. 713 (2002) 713–718.
[26] E. Weetjens, X. Sillen, E. Valcke, Mater. Res. Soc. Symp. Proc. 932 (2006) 735–742.
[27] N. Mokni, S. Olivella, X. Li, S. Smets, E. Valcke, J. Phys. Chem. Earth 33 (suppl. 1) (2008) S436–S443.
[28] N. Mokni, S. Olivella, X. Li, S. Smets, E. Valcke, A. Mariën, J. Nuc. Mater. 404 (2) (2010) 144–153.
[29] U. Berner, Waste Manag. 12 (1992) 201–219.
[30] A. Mariën, E. Valcke, N. Bleyen, M. Van Geet, M. Wevers, The use of μCT and ESEM in the study of the osmosis-induced water uptake by Eurobitum bituminized radioactive waste, in preparation.
[31] H.R. Beyers, p. 24 in 'Elements of Cloud Physics', University of Chicago Press, 1965, 199 p.
[32] R.C. Hoffman, A. Laskin, B.J. Finlayson-Pitts, Aerosol Sci. 35 (2004) 869–887.